Chemistry and Materials Research
ISSN 2224- 3224 (Print) ISSN 2225- 0956 (Online)
Vol.7 No.8, 2015
www.iiste.org

Phosphorus Desorption Study Using Dialysis Membrane Tube Filling Fe-Al-Mn Ternary Mixed Nanocomposite from Different Farming Practice of Acidic Soil

[1]Gemechu Shumi Bekesho[1], Abi Tadasse Mengesha[2], Tesfahun Kebede[2]
1, Bako Agricultural Research Center of Oromia Agricultural Research Institute, Bako, Ethiopia
PO box 03, Bako Agricultural Research Center, Ethiopia
2, Department of Chemistry, College of Natural and Computational Sciences, Haramaya University, Haramaya, Ethiopia

Abstract
Knowledge of the effect of the P remaining in the soil (residual effect) is of great importance for fertilization recommendation. Environmental applications of nanotechnology address the development of solutions to the existing environmental problems, preventive measures for future problems resulting from the interactions of materials with the environment. For this purpose, Fe-Al-Mn ternary mixed oxide nanocomposite adsorbent with 70, 25 and 5 percentage composition of Fe, Al, Mn respectively was synthesized by impregnation method. Its crystal structure was hematite with 20.31 nm size and 69.93 m^2/g surface area. The study of phosphate desorption was carried out on different farming practices with four types of treatments: Sole Maize conventional practice (SMCP), Sole Maize conservational agriculture (SMCA), Sole Haricot bean conservation agriculture (SHCA) and Maize-Haricot bean intercropping conservation agriculture (MHCA). The simulation of phosphate desorption from soil to plant was predicted by dialysis membrane tube filled with the ternary mixed nanocomposite (DMT-FeAlMn). DMT-FeAlMn was founded to be the promising adsorbent to simulate the plant–phosphate relation in acidic soil or to estimate the properties of soil for phosphate desorption to the soil solution. The observed desorbed of phosphate was significant in the treatment order of SMCP < SHCA < SMCA < MHCA. The releasing rate of phosphate from soil followed first order kinetics having SMCP (R^2 = 0. 996), SMCA (R^2 = 0.997), SHCA (R^2 = 0.993), and MHCA (R^2 = 0.991) with rate constant 0.0006hr^{-1}.
Keywords: Desorption, Nanosized Fe-Al-Mn mixed oxide, Residual soil-phosphate, Farming practice

1. Introduction

Phosphorus is commonly a limiting nutrient for plant growth in many soils around the world (McDowell and Stewart, 2006). The amount of P removed from a field by crops in general varies from 3-33% of applied P fertilizer (Kamper & Claassens, 2005). Soils receiving successive applications of fertilizer P or manure over a long-term, therefore, can accumulate large amounts of residual P. This represents not only an uneconomic practice, as phosphate ores are expected to be depleted within approximately 50 years, but also the risk of potential for P loss to surface waters via overland or subsurface flow and intern accelerate freshwater eutrophication (McDowell & Sharpley, 2002).

The P availability for plants is usually done using single chemical extraction methods. However, it is accepted that the plant acquires its P from the soil solution that has to be replenished over the growth period. The availability of P to plants therefore depends, among other things, on the rate at which it is released to replenish the soil solution (Raven and Hossner, 1994). Due to P build up with a significant residual effect could be expected and this can lead to an underestimation of the available P if not taken into account.

Plant P availability of residual P in soils can be reliably estimated by successive cropping experiments carried out in field or green house conditions, where P is taken up until P deficiency occurs or a response to added P is measured (Indiati, 2000). This approach, however, takes many years to realize which makes it very expensive and time consuming. Therefore, instead of attempting to tap the residual P by continually cropping till the plant responds, more rapid soil test methods that can approximate this biological measure have been required. According to these methods, a given soil is subjected to successive P desorption using materials that can act as P sinks (Van der zee *et al*., 1987). By employing these methods, one can study the P release rate of a given soil and for how long a given soil can supply P. This in turn enables to know for how long it will take for soil P to deplete to a concentration where manure or fertilizer P can again be applied (Freese *et al.,* 1995; Lookman *et al*., 1995).

In order to assess long-term P desorption kinetics, it is necessary to sufficiently supress the backward resorption reaction. This can be done by introducing effective P sinks into the system. Van der zee *et al*. (1987), proposed the use of Fe-oxide impregnated filter paper strips (Fe-oxide strips) as a promising method to study the P release kinetics of soils. Acting as a sink for P, the Fe-oxide strips have a sounder theoretical basis than the chemical extractants in estimating available soil P (Sharply, 1996). However, this method was found to be not well applicable for long-term desorption studies as it may lead to errors due to adhesion of fine P-rich particles to the paper strips and due to the mechanical instability of the paper when used for long term desorption studies

(Freese *et al.,* 1995; Lookman *et al*., 1995). Recently, use of dialysis membrane tube filled with hydrous ferric oxide (DMT-HFO) in place of resin/Fe-oxide paper strips for studying long-term P dynamics has been proposed (Ochwoh *et al*., 2005; Taddesse *et al*., 2008). This method is similar to Fe-oxide impregnated filter paper strips but in this case the HFO is placed in a dialysis membrane tube instead of being impregnated in the filter paper. This has the advantage of not allowing strong chemicals to come into contact with the soil. This system is mechanically stable and capable of maintaining low P activity in solution for longer period of time, and, therefore, P release over long periods of time can be measured in a more natural environment than the routine soil tests (Freese *et al*., 1995; Lookman *et al*., 1995).

The phosphate sink in all the aforementioned cases however is hydrated ferric oxide which is an example of typical single component system. Such systems in amorphous and nanocrystalline form have been emloyed widely for phospate sorption acting as sinks. On the other hand, different Fe_2O_3 as natural minerals exist in our natural environment usually not alone and they very often coexist with silicate and alumina in soil. The fraction of silicate and alumina in clay varies in a broad range from very low up to 75% (Li *et al*., 2007). Multi-component sorbents comprising mixtures of metal oxides, clay, quartz and organic compounds are ubiquitous in soils and aquatic environments and have been shown to be significant in determining the environmental distribution of various contaminants and nutrients (Sujana and Anand, 2010).

In view of the above facts, DMT-HFO was improved by using the mixed Fe-Al-Mn oxide nanocomposite, when placed in the dialysis membrane tube mimics (simulate) better the plant mode of action than the single component system due to high surface area of Fe-Al mixed oxides (Zhao *et al.*, 2010) and important scavenging property of Mn oxides(Davies and Morgan, 1989). Generally, the objective of this study was to study the desorption of p in acidic soil under different type of farming practice by filling the as-synthesized adsorbent Ternary mixed nano composite (Fe-Al-Mn) in dialysis membrane tube(DMT).

2. Experimental site and procedure

2.1. Description of experimental site

The study area of experiment was carried out at Bako Agricultural Research Centre (BARC) on best bet conservation farming practices, which are four treatments; these have been going on since 2010 to 2013. The centre is located in the western part of Ethiopia at about 9^0 6'N latitude and 37^0 9' E longitudes; it is about distance of 250 km away from Addis Ababa at an altitude of 1650 m above sea level. It has a warm humid climate with annual mean minimum, mean maximum and average temperatures of 14, 28 and 21^{o}C respectively as recorded in 1990-2014. The area receives an annual rain fall of 1237mm from May to October with maximum precipitation in the month of June to August (BARC metrological data record). The soil of the area is characteristically reddish brown with a pH that falls in the range of slightly acidic to very acidic (BARC soil laboratory record).

Synthesis of Fe-Al-Mn mixed nanocomposite and the desorption experiments using the as-synthesized material was carried out at Haramaya University, Chemistry Department research laboratory. XRD was carried out for structural characterization at the Geological survey of Ethiopia. Infrared spectroscopic study was conducted for identification of functional groups at Addis Ababa University, and UV-Vis spectroscopic technique was used at Chemistry Department research laboratory of Haramaya University

2.2. Experimental Procedures

2.2.1. Synthesis of Fe-Al-Mn mixed oxide nanocomposite

The Fe-Al-Mn Ternary mixed oxides nanocomposite was prepared by impregnation method (**Aguila *et al*., 2008**). In which 0.1 molar nano sized Fe-Al-Mn ternary mixed oxides was prepared by impregnating MnO_2 with aluminum nitrate nona-hydrated ($Al(NO_3)_3.9H_2O$, 98 %, Hightech Health care, India), ferric nitrate nona-hydrate ($Fe(NO_3)_3.9H_2O$ 98 %, Hightech Health care, India) solution in deionized water with 1:3 ratios. Three samples of the adsorbent having different molar percentages of iron, aluminum and manganese precursors as (90, 8, 2), (80, 10, 10), (70, 25, 5) % or molar ratio 45:4:1, 8:1:1 and 14:5:1, respectively, were prepared for this study. During synthesizing process, three beakers (1L) were needed. The amount of Al and Fe nitrates were dissolved completely in separate beakers. They were mixed together in a third beaker while stirring after complete dissolution. The MnO_2 powder was added on the mixed salt solution. The samples were left for 6 hr without disturbance then after dried at 110^{o}C in an oven over night and waited until complete drying and further calcined in mulfurnace at 400^{o}C for 4 hr.

2.2.2. X-Ray Power Diffraction Characterization of the As-Synthesized Adsorbent

X-ray diffractmeter (XRD, D8-Advanced, Germany, power 40 kW with 35 mA at 25^{o}C) was used to determine the X-ray diffraction (XRD) pattern of the adsorbent from which to determine the phase composition and estimate the crystallite size of the powders**.** The size of the primary crystallite (D_s) of the solid-phase (Fe_2O_3-Al_2O_3-MnO_2) was calculated from the XRD diffractometry according to the Dubye Scherrer equation (**Laurent *et al*., 2008**):

$$D_s = \frac{0.9\,\lambda}{\beta\,\cos\theta} \quad (1)$$

Where, D_s is mean crystallite size (nm), λ wavelength of the incident radiation (λ = 0.15405 nm), β pure diffraction broadening (radians) and θ the Bragg angle (degrees, half-scattering angle). Usually β is taken as the full width at half maximum of the major diffraction band (FWHM).

2.2.3. Determination of surface area

The specific surface area of adsorbent powder was determined by using the Sear's methods. In which 0.5 gram of the adsorbent powder, 10.0 g of sodium chloride (NaCl 99.5% BDH chemicals Ltd Poole, England) and 50 mL volume of distilled water were added in each beaker and then acidified with 0.1M hydrochloric acid (HCl, 36-37%, BDH chemicals Ltd, England) to pH value of 3-3.5. Titrations were carried out using 0.1 M of sodium hydroxide (NaOH, 97.5% BDH chemicals Ltd, England) to adjust the pH first to 4.0, and then increase it to pH value of 9.0. The Volume, V (mL) required to raise the pH from 4.0 to 9.0 was noted and the specific surface area was computed from the equation (2) (**Sears, 1956**).

S (m^2/g) = 32V-25 **(2)**

2.2.4. FTIR Characterization Fe-Al-Mn Ternary mixed oxide Nanocomposite

To determine bond structure of synthesized and selected Fe-Al-Mn sample, FTIR Spectrometer (FTIR-65, Perkin-Elmer) was used. First, at room temperature, the instrument was adjusted with a resolution of 4 cm^{-1}, accumulating 100 scans, between 400 cm^{-1} and 4000 cm^{-1} wave numbers. Second, 0.001 g of each sample was mixed with 0.1 g of KBr and ground to a fine powder, respectively. Then, a transparent disc was formed using a nitrogen pressure in moisture free atmosphere for 1 h and absorption was recorded (**Li *et al.*, 2007**).

2.2.5. Elemental Characterization of Fe-Al-Mn Ternary mixed oxide Nanocomposite

Percentages of each metal in Fe-Al-Mn were determined by Flame Atomic Absorption Spectrophotometer (FAAS, Model 210/211, Karisruh, West Germany). For this purpose, 0.5 g of the as-synthesized powder for three replication were digested with a mixture of concentrated nitric acid (7 mL), concentrated hydrochloric acid (4 mL) and hydrogen peroxide (2 mL) using acid digestion tube till clear solution appeared. The samples were transferred to 100 ml volumetric flasks and brought to volume using deionized water. 1 mL of this solution was diluted further to 50 mL and the concentration of iron was read from the solution in 50 mL volumetric flasks. The results were corrected for the dilution factor (**Bock, 1978**). Similarly, the standard solutions were prepared from the precursors ($Fe(NO_3)_3.9H_2O$, $Al(NO_3)_3.9H_2O$ and MnO_2) from which the results were calculated.

2.2.6. Desorption Study

A desorption study was carried out using dialysis membrane tubes (Visking, size $3^{20/32}$ inches, approximate pore size 2.5-5.0 nm; membrane thickness 3 µm, MWCO 12000 kDa) filled with hydrous ferric oxides as described by **Freese *et al.* (1995)**. Al-Fe-Mn mixed nano oxide(20.3 nm in size, 69.8 m^2/g of surface area) was used instead of Fe_2O_3. The 0.15 m of DMT strip was filled with 20 mL of 0.1 gram Fe-Mn-Al oxide nanoparticle (sorbent), 0.5 M HCl or NaOH was added in drops to adjust the mixture to the pH (KCl) of the soils (Table 3.4) and closed with a nylon thread on both ends. The sorbent suspension was stirred vigorously during the filling. The FeAlMn-DMT were placed in 200 mL polyethylene containers with 1g of soil and 80 mL of 2 *mM* $CaCl_2$ and 0.3 *mM* KCl solution. All the experiments were carried out in complete randomized design (CRD) having three replication. The polyethylene containers were continuously shaken for 28 days on an end-over-end shaker at 120 oscillations per minute (opm). It was found in a preliminary investigation that shaking at 120 opm created the required perturbance yet the tubes could be shaken for 14 days without physically damaging the dialysis tubes (**Taddesse *et al.*, 2008**). On each of seven days intervals: 1, 7, 14, 21 and 28, the DMT- FeAlMn was replaced with new DMT-FeAlMn. In doing so, a glass rod was used to remove any attached soil from the dialysis membrane tubes. At each time interval, three of the tubes were removed, opened and the contents transferred to glass bottles. P in solution was determined calorimetrically with the 0.1 M NaOH and molybdophosphoric blue method using ascorbic acid as a reductant. A series of standard and blank were prepared with the same background FeAlMn.

2.2.7. Data Analysis

To compare the effects of the treatments statistical analysis of general linear model (GLM) was carried out to determine the existence of any statistical difference among the treatments. Separations of significant differences between and among treatments mean were made by SAS software (SAS, 9.3version).

3. Result and discussion

3.1. XRD patterns Characterization as-synthesized Absorbent Nanoparticles

The x-ray diffraction study of the as-synthesized Al-Fe-Mn mixed oxide nanoparticle powder was carried out with Bruker D8 Advance X-ray diffractometer (XRD). The XRD pattern was obtained through a Cu target K_α radiation (λ = 0.15405 nm and θ = 4 - 64°). As shown in **Table 3.1**, the alpha (α) average crystallite size of the XRD patterns was determined using Debye Scherrer's (equation 1).

As shown in Figure 3.1, the hematite crystals were formed in all samples powder. The 2θ values from each the x-ray diffraction (XRD) Patterns: 90-8-2 (24.6, 33.652, 36, 41.3, 49.8, 54.6, 58 and 62.9) ^{o}, 80-10-10 (24.3, 26.7, 33.298, 35.8, 41, 49.5, 54.3, and 62.5) ^{o} and 70-25-5 (24.5, 26.9, 33.497, 36, 41.1, 49.5, 54.3, and 62.8) ^{o} were observed and of these 33.652^{o}, 33.298^{o} and 33.497^{o} respectively are observed as highest peaks.

Despite that the iron oxides take the magnetite, maghemite and the hematite crystalline phase, the XRD pattern of all the as-synthesized ternary oxides nanoparticle (which were calcinated at 400^{o}C for 4 hrs) typically showed only the hematite phase (Figure 3.1). This contrasted earlier reports that in the dry state, γ-Fe_2O_3 (Maghemite) phase usually transforms to α-Fe_2O_3 (hematite) phase when heated at temperatures ranging from 370-600°C for 2 hr (Martinez *et al.,* 1998). Also for lower initial iron concentration, pure maghemite phase was formed at a calcination temperature of 500°C and the maghemite phase transformed completely into rhombohedral hematite at a calcination temperature of 850^{o}C for two hours (Sahoo *et al.,* 2010) and with increasing of the calcination temperature, the crystal size of the nanosorbent increases (Gaber *et al.,* 2014). There also influences of the calcining temperature and calcining time on the crystallite size, crystallinity, and lattice parameters reported by Zhong *et al*. (2012) that as calcining time increased, the crystallite size and the crystallinity were increased.

The data does not show any Al and Mn presence because they may entered into Fe oxide lattice as their small ionic radius size. Shannon *et al*., (1976) and Tesfa Oluma *et al*., (2014) reported that the ionic radii of Fe^{+3}, Al^{+3} & Mn^{+4} for coordination number 6 are 59 pm, 54 pm & 53 pm, respectively. In other word, the large amount of Fe loaded into the system during synthesis may cause insignificance of Al and Mn on the XRD data.

Furthermore, the diffraction peaks found were the characteristic peaks of Fe_2O_3 (hematite) this may due to small percentage of MnO_2 dominated by Fe_2O_3 and alumina should be amorphous structure. In fact, crystallized alumina such as γ-Al_2O_3 might present under thermal treatment at 800 ^{o}C and α-Al_2O_3 might present under thermal treatment at 1000 ^{o}C (Shaheen and Hong, 2002). Mn and Al oxides were hardly detected in the XRD pattern and this may occur due to the presence of Mn and Al oxides in the adsorbent might be insignificant or the formation Al-Fe-Mn solid solution might have forced the Mn and Al species to occupy interstial holes created by the crystal lattices of α-Fe_2O hematite (Shihabudheen *et al,*. 2006).

Table 3.4. Particle sizes of the as-synthesized of FeAlMn mixed oxide of different % composition

S.N	Sample Code	FWHM(β)	β in Rad.	2θ	Cosθ (rad.)	D_s (nm) size of particles
1	**GS_HU_*70_25_5***	0.399	0.006964	33.497	0.957579	20.31
2	**GS_HU_*80_10_10***	0.367	0.006405	33.298	0.958078	22.07
3	**GS_HU_*90_8_2***	0.356	0.006213	33.652	0.957188	22.77

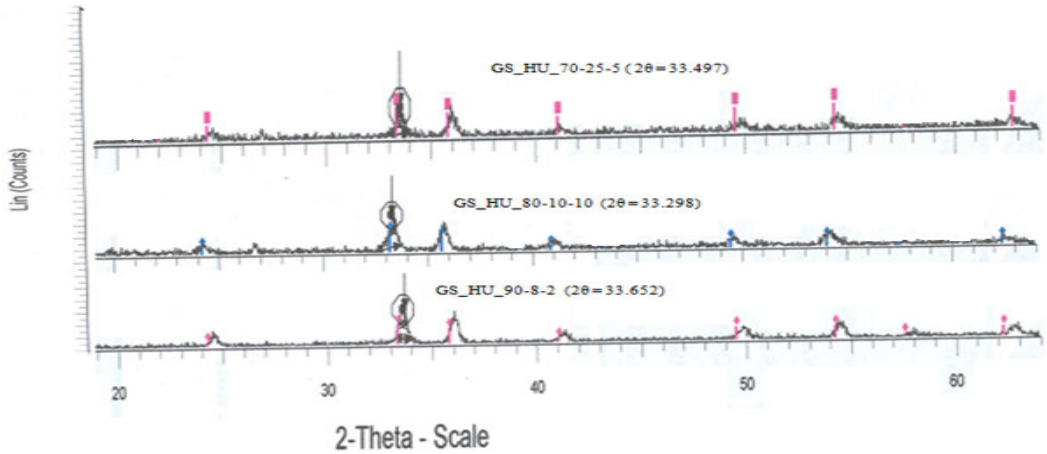

Figure 3.1. XRD patterns of Fe-Al-Mn as-synthesized nanocomposites of different % compositions

3.2. Surface area Characterization as-synthesized Absorbent Nanoparticles

Table (3.2) shows the specific surface area of as-synthesized mixed oxide powders as computed from the results of potentiometric titration. The volume of NaOH required to raise the pH from 4.0 to 9.0 was noted and the specific surface area was calculated by equation (7). The specific surface area was founded to be in the order 70:25:5 > 80:10:5 > 90:8:2. The ternary oxide with the smallest size was found to exhibit the largest specific surface area. Gulshan *et al*. (2009) and Cava *et al*. (2007) observed similar trend. This is due to the influence of content of aluminum variation excited in the specific surface areas of the as-synthesized powders (Cava *et al*., 2007). As it can be seen the sample with (70, 25 and 5) % composition of Fe, Al and Mn shows greater specific surface area and smaller particle size.

Nano-materials with high surface activity, high specific surface area and high surface energy, show promising potential in the preparation of high performance adsorption and thus are widely used as adsorbents (Wang *et al.*, 2004, 2006). As result of these specific properties of nanoparticles, the as synthesized sample, GS_HU_70_25_5, was selected for further characterization by FAAS and FTIR. Also because of its high specific surface area and small size, studies involving phosphate desorption from the soil were carried out making use of this sample.

Table 3.5. Specific surface area of as-synthesized powders

S.N	Sample Code	Volume(mL) of 0.1 NaOH to raise pH 4-9	Specific surface area (m^2/g)
1	**GS_HU_*70_25_5***	3.2	69.93±1.84
2	**GS_HU_*80_10_10***	1.7	29.40±3.20
3	**GS_HU_*90_8_2***	1.3	15.53±1.84

3.3. Elemental analysis of as-synthesized absorbent nanoparticles

Elemental content of the selected adsorbent is GS-HU-*70-25-5* was analyzed through FAAS. The obtained result pertaining to the percentages of iron, aluminum and manganese oxides are shown in Table 3.3. The analysis was performed using a standard solution of each analyte prepared at a series of concentrations. The as-synthesized mixed oxide powder was dissolved by acid digestion method, in which 0.5 g of the sample was dissolved in 100 mL volumetric flasks using a mixture of acids with appropriate concentrations volume ratios. The unknown concentrations of metal percentages were calculated using linear equation from its calibration plot prepared from series of concentrations of standard versus the corresponding absorbance reading (Figure 3.2, 3.3 and 3.4). The FAAS result indicated (Table 3.3) that the percentage composition of Fe, Al and Mn in the as-sythesiized selected nanosorbent was found to be 68.37, 24.0 and 3.56, respectively and this is not far from the theoretical composition.

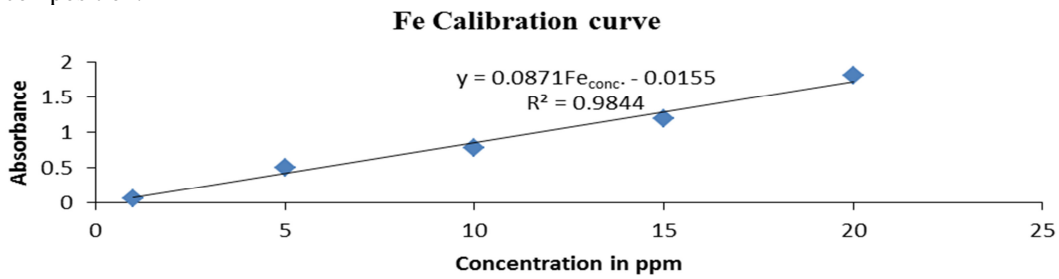

Figure 3.2. Calibration curve for Fe in as synthesized adsorbent (FAAS reading).

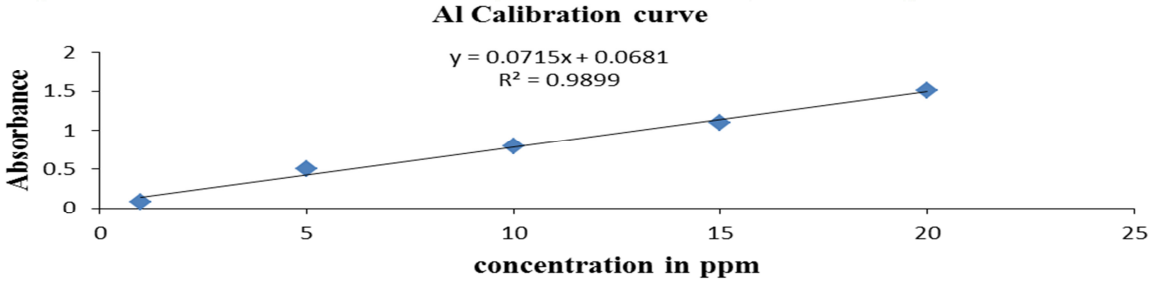

Figure 3.3. Calibration curve for Al in as synthesized adsorbent (FAAS reading).

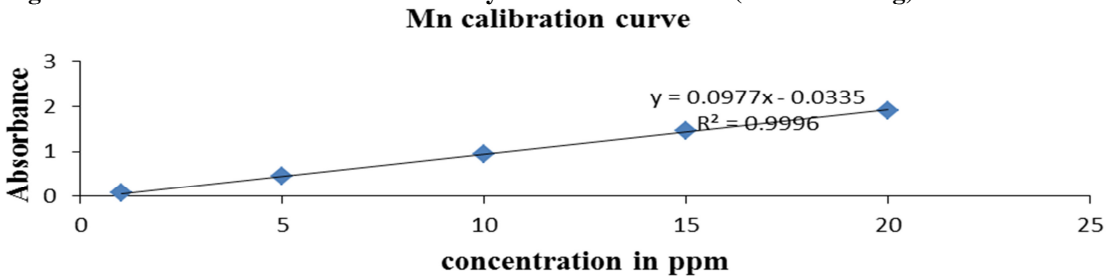

Figure 3.4. Calibration curve for Mn in as synthesized adsorbent (FAAS reading).

Table 3.6 Actual yield and theoretical composition the of selected as-synthesized adsorbent

Sample code	Element	Theoretical composition (%)	Actual yield (%)
GS-HU-70-25-5	**Fe**	70	68.37±0.85
	Al	25	24.01±1.12
	Mn	5	3.56±0.03

3.4. Infrared Spectroscopic Characterization as-synthesized Absorbent Nanoparticles

The FT-IR spectrum of the selected Al-Fe-Mn (GS_HU_70-25-5) mixed oxide sample was carried out in KBr medium and the results obtained as such are depicted on Figure 3.4 with the main absorption peaks located 3400, 1628, 545 and 474 cm^{-1}. Accordingly, the absorption peaks at 3400 and 1628 cm^{-1} are assigned to symmetrical stretching and bending vibration of the O-H group, respectively (Sujana and Anand, 2010). The bending vibrations of the O-H group may actually be attributed to the presence of physiosorbed water on the surface oxides. The bands at 545 cm^{-1} and 474 cm^{-1} are assigned to the symmetrical stretching vibrations of the mixed metal oxides M-O and M-M-O, respectively (Zhang *et al.*, 2009).

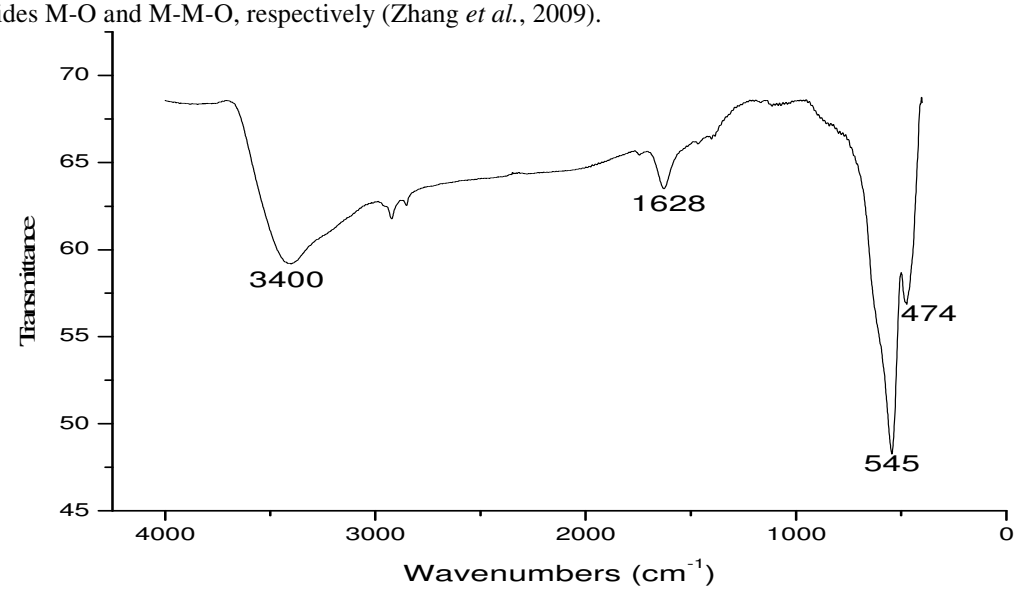

Figure 3.5. FTIR Spectrum of the selected nano sized Fe-Al-Mn mixed oxide adsorbent (GS-HU-70-25-5).

3.5. Phosphate Desorption Study

The study pertaining to phosphate desorption was carried out using the DMT-FeAlMn mixed oxide nano composite particle on four treatments having different management practices: sole crop, intercropping and tillage practice.

The amount of P desorbed by DMT-FeAlMn was significantly influenced ($\alpha = 0.05$) both by the treatments and extraction time (Table 3.5). The cumulative P desorbed was higher in the Maize-Haricot Bean intercropping Conservation Agriculture (MHCA) (1.97-14.26 mgkg $^{-1}$) and lower in the sole maize conventional practice (SMCP) (1.36 -9.583 mg kg^{-1}) at all levels of extraction time (1 –28 days). In this study, Sole Maize Conservation Agriculture (SMCA) (1.7 – 11.56 mg kg^{-1}) and Sole haricot bean Conservation Agriculture (SHCA) (1.76 – 10.56 mg kg-1) treatments resulted in a comparable amount of extracted P at all levels of extraction time. Cumulative P released with time followed, in general, the same pattern for all treatments. All the treatments showed an increasing trend for the period studied in this experiment (28 days). This trend is observed in contrast to the previous reports (Freese at al., 1995; de Jager and Claassens, 2005; Taddesse *et al*., 2008). In the reports, the authors found two distinct pools of soil P within 56 days, one with rapid release kinetics and the other with slower desorption kinetics. The fast P pool presumably represents P bound to reactive surfaces, directly in contact with the aqueous phase. The slow P release rate from the second pool is either the result of slow dissolution and/or diffusion kinetics from interior sites inside oxyhydroxide particles (McDowell and Sharpley, 2003).

Desorption kinetics of soil as determined using the DMT-FeAlMn as the sorbent can be schematically represented as shown equation (3)

$$SP \xrightarrow{k_R} P_{sol} \xrightarrow{k_t} P_{FeAlMn} \qquad (3)$$

Where SP is the solid phase P, P_{sol} is P in solution, P_{FeAlMn} is P adsorbed by FeAlMn, k_T is the rate constant of P

transport through the membrane, and k_R is the rate constant of P release. The presence of two pools is assumed: the pool with the fast release kinetics is pool A (SP_A) and the pool with the slow release kinetics is pool B (SP_B). With this assumption, the mass balance equation for the total exchangeable solid phase soil P (SP_{total}) at time t = 0 is:

$$SP_{total\ 0} = SP_{A0} + SP_{B0} \quad (4)$$

Where SP_{A0} is initial amount of P in pool A and SP_{B0} is initial amount of P in pool B. The mass balance equation at time **t** will therefore be:

$$SP_{total\ (t)} = SP_{A(t)} + SP_{B\ (t)} \quad (5)$$

Assuming the decrease in SPA and SPB follow first order kinetics, the integrated rate laws for the decrease of SP_A and SP_B will be:

$$SP_{A(t)} = SP_{A0}\, e^{-k_A t} \text{ and } SP_{B(t)} = SP_{B0}\, e^{-k_B t} \quad (6)$$

Where k_A and k_B are conditional first order rate constants (day $^{-1}$) for P desorption from pools A and B respectively.

The total solid phase soil P ($SP_{total\ (t)}$) remaining at time t will be given by:

$$SP_{total\ (t)} = SP_{A0}\, e^{-k_A t} + SP_{B0}\, e^{-k_B t} \quad (7)$$

The total amount of P released at time t is expressed as:

$$\begin{aligned} P_{R(t)} &= SP_{A0} - SP_{A\ (t)} + SP_{B0} - SP_{B\ (t)} \\ &= SP_{A0} - SP_{A0}\, e^{-k_A t} + SP_{B0} - SP_{B0}\, e^{-k_B t} \\ &= SP_{A0}\,(1 - e^{-k_A t}) + SP_{B0}\,(1 - e^{-k_B t}) \end{aligned}$$

It was assumed that the rate constant of P release from the soil was equal to the rate constant of P adsorption (k_A) by the DMT-FeAlMn. The rate constant of P adsorption (k_A) by the DMT-FeAlMn was obtained from a plot of the natural logarithm (ln) of the P adsorbed by the DMT-FeAlMn against time with the slope as k_A.

For a long term desorption study (28 days), one might expect the two pools, pool A and pool B to play their role. However, in this study only rapid release of P was observed this shows the soil solid phase releasing of phosphorus to the solution is only from pool A as the release of P still fast. This is probability because we used in our study a strong sorbent (Fe-Al-Mn ternary system) than the previous studies (Freese *at al*., 1995; de Jager and Claassens, 2005; Taddesse *et al*., 2008) where only single system (hydrated ferric oxide-HFO) was employed for similar purpose.

As depicted in (Figure 3.6.) the desorbed of P of the treatments were linearly high significant which have SMCP (R^2 = 0. 996), SMCA (R^2 = 0.997), SHCA (R^2 = 0.993), and MHCA (R^2 = 0.991). However, the two kinetics, fast and slow releasing P were expected, only fast kinetics occurred is due to the experimental days were not enough to attain both the kinetics. As shown (Figure **3.7.**) the p desorption kinetic of soil was found to follow first order model (first order kinetic) which schematically showed at equation (3):

$$\mathbf{SP_{A(t)} = SP_{A0}\, e^{-k_d t}}$$

Where k_d is the rate of the desorption P was founded 0.0006 hr^{-1} in this studies. **Taddesse *et al.* (2008)** have reported comparable result (0.00034-0.0004 hr^{-1}) under the studies of kinetics of residual phosphate desorption from long-term fertilized soils of South Africa. The cumulative desorption of P extracted by DMT-FeAlMn within 28 days was very low as compared to the total P, but it is larger as compared to the availability of P (table 3.3 and 3.4).

Table 3.4. Selected physical and chemical properties of the soil samples studied

		Treatments						
Parameters		**SMCP**	**SMCA**	**SHCA**	**MHCA**	**CV**	**LSD**	**SL**
pH (1:2.5)	**H_2O**	4.85^a	4.76^b	4.67^c	4.53^d	0.55	0.052	**
	KCl	3.62^a	3.56^c	3.57^b	3.51^d	0.09	0.0067	**
Av.P	**mg Kg^{-1}**	9.50^b	8.97^b	8.39^b	35.97^a	8.87	2.78	**
TP		1580.3^a	1629.9^a	1642.4^a	1654.7^a	2.61	85.01	NS

*Av.P = Availability of P, TP = Total phosphorus, NS = non-significant, SL=significant level, CV = Coefficient of Variance, LSD = least significance difference, Significance level, ** ($P \leq 0.01$), *($P < 0.5$) NS ($P > 0.05$)*

Table 3.5. Desorption of phosphorus from soil (for 28 days)

Treatment	Days					
	1	7	14	21	28	CDP (mgkg^{-1})
SMCP	z1.36^{c}	y3.22^{b}	x5.44^{c}	w7.98^{c}	v9.58^{d}	27.58
SMCA	z1.70^{b}	y3.37^{ab}	x6.27^{b}	w8.93^{b}	v11.56^{b}	31.83
SHCA	z1.76^{b}	y3.13^{b}	x5.46^{c}	w8.28^{c}	v10.65^{c}	29.27
MHCA	z1.97^{a}	y3.58^{a}	x7.977^{a}	w10.98^{a}	v14.26^{a}	38.78
CV	2.33	4.72	2.7	2.41	2.5	
LSD	0.0789	0.3138	0.339	0.435	0.575	
SL	**	NS	**	**	**	

*NS = non significant, SL = significant level, CV = coefficient of variation, LSD = least significance difference, CDP = cumulative desorption P, Significance level, ** (α ≤ 0.01), *(α < 0.05) NS (α > 0.05), Mean values in rows with different letters v, w, x, y and z are significantly different, Mean values in columns with different letters a, b, c and d are significantly difference.*

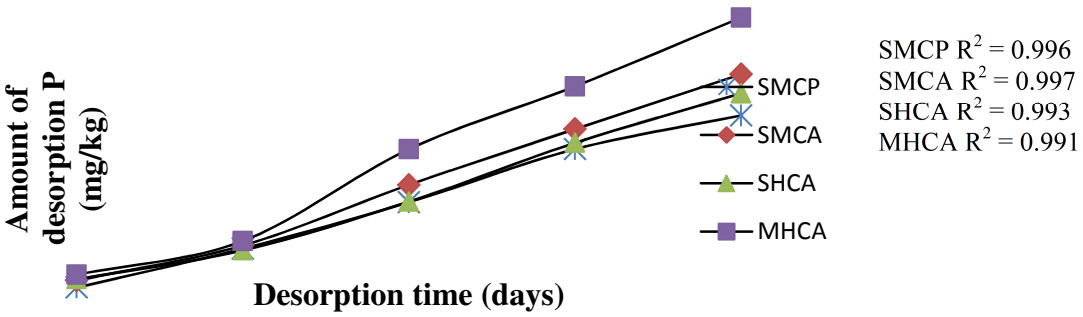

Figure 3.6. Cumulative desorbable P with time extracted using DMT-FeAlMnO for the different treatments over 28 days.

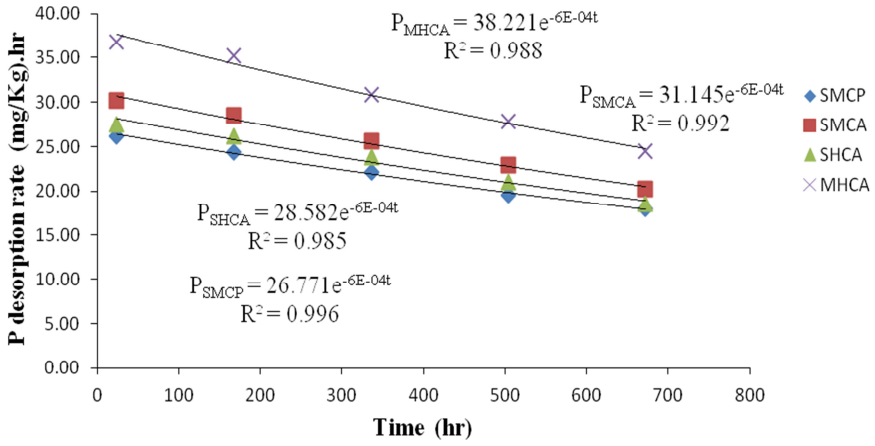

Figure 3.7. Phosphorus desorption rate from soil to solution.

4. Conclusion

The FeAlMn mixed oxide nanocomposite was synthesized using impregnation method and studies of adsorption properties were carried out to mimic the plant to absorb the phosphate from soil having different management with almost the same rate of fertilizer applied. The as-synthesized adsorbent was hematite (Fe_2O_3) structure with 20.31 nm crystalline size and 69.93 m^2/g surface area.

According to this study, cumulative P released with time followed the same pattern for all treatment of soils, with rapid release of P with 28 days. Only fast releasing of P was attained during the experimental periods and no desorption stable phase was reached during the entire period of extraction time, indicating that desorption can continue for a longer period than 28 days.

P desorption kinetics were described relatively well by first-order model (R^2 = 0.996, 0.992, 0.985 and 0.988 of SMCP, SMCA, SHCA and MHCA respectively). The total P extracted varied among treatments

following the order: SMCP< SHCA < SMCA < MHCA. The rates of desorption for all treatments were the same 0.0006 hr^{-1} for all treatments indicating that chemical and physical properties among the treatments are almost the same.

6. Reference

Aguila, G., F. Gracia, and P. Araya. CuO and CeO_2 catalysts supported on Al_2O_3, ZrO_2, and SiO_2 in the oxidation of CO at low temperature. *Applied Catalysis A*, 343(1): 16-24.

Bock, R.A. 1978. Handbook of Decomposition Methods in Analytical Chemistry. International Textbook Co., Glasgow, Scotland, 458p.

Cava, S., S.M. Tebcherani, I. A. Souza, S.A. Pianaro, C.A. Paskocimas, E. Longob, and J.A. Varela, 2007. Structural characterization of phase transition of Al_2O_3 nanopowders obtained by polymeric precursor method. *Materials Chemistry and Physics*, 103: 394-399

Davies, S. H. and Morgan, J. J, 1989. Manganese (II) oxidation kinetics on metal oxide surfaces, *Journal of Colloid and Interface Science*, 129(1): 63-77.

de Jager, P. C. and Claassens, A. S., 2005. Long - Term Phosphate Desorption Kinetics of an Acid Sandy Clay Soil from Mpumalanga, South Africa. *Communications in Soil Science and Plant Analysis*, 36(1-3): 309-319.

Freese, D., R. Lookman, R. Merckx, and W.H. van Riemsdijk, 1995a. New method for the assessment of long-term phosphate desorption from the soil. *Soil science of American Journal,* 59: 1295-1300.

Gaber, A., M. A. Abdel- Rahim, A. Y. Abdel-Latief, and M. N. Abdel-Salam, 2014. Influence of Calcination Temperature on the Structure and Porosity of Nanocrystalline SnO_2 Synthesized by a Conventional Precipitation method. *International Journal of Electrochemical Science*, 9: 81-95.

Gulshan, F., Y. Kameshima, A.Nakajima, and K.Okada, 2009. Preparation of alumina–iron oxide compounds by gel evaporation method and its simultaneous uptake properties for Ni^{2+}, $NH4^{+}$and $H_2PO_4^{-}$. *Journal of Hazardous Materials*, 169: 697-70.

Indiati, R., 2000. Addition of phosphorus to soils with low to medium phosphorus retention capacities. II. Effect on soil phosphorus extractability. *Communication of Soil Science Plant Analysis,* 31: 2591-2606

Kamper, M. *and Claassens, A.S., 2005.* Exploitation of soil by roots as influenced by phosphorus applications. *Communication Soil Science and Plant Analysis*, 36: 309-319.

Laurent, S., D. Forge, M. Port, A. Roch, C. Robic, L. V. Elst and R.N. Muller, 2008. Magnetic iron oxide nanoparticles: synthesis, stabilization, vectorization, physicochemical characterizations, and biological applications. *Chemical Review,* 108: 2064-2110.

Li, F.B., X.Z. Li , C.S. Liu, T.X. Liu, 2007. Effect of alumina on photocatalytic activity of iron oxides for bisphenol A degradation. *Journal of Hazardous Materials,* 149: 199-207.

Lookman, R., D.Freese, R. Merckx, , K. Vlassak, and W.H. van Riemsdijk, 1995. Long-term kinetics of phosphate release from soil. *Environmental Science & Technology*, 29(6): 1569-1575.

Martinez, B., X. Obradors, Ll. Balcells, A. Rouanet, and C. Monty, 1998. Low Temperature Surface Spin-Glass Transition in γ -Fe2O3 Nanoparticles. *Physical Review Letters*, 80(1): 181-192.

McDowell, R. and Sharpley, A., 2003. Phosphorus solubility and release kinetics as a function of soil test P concentration. *Geoderma*, 112(1): 143-154.

McDowell, R.W, and Sharpley, A., 2002. Phosphorus transport in over land flow in response to position of manure application. *Journal of Environmental Quality,* 31:217-227.

McDowell, R.W. and Stewart, I., 2006. The phosphorus composition of contrasting soils in pastoral, native and forest management in Otago, New Zealand: Sequential extraction and ^{31}P NMR. *Geoderma*, 130(1-2): 176-189.

Ochwoh, V.A., A.S. Claassens, and P.C. De Jager 2005. Chemical changes of applied and native phosphorus during incubation and distribution into different soil phosphorus pools. *Communication Soil Science and Plant Analysis*, 36: 535-556.

Raven, K.P. and Hossner, L.R., 1994. Sorption and desorption quantity intensity parameters to plant available soil phosphorus. *Soil Science Society of America Journal, 58: 405 - 410.*

Sahoo, S.K., K. Agarwal, A.K. Singh, B.G. Polke and K.C. Raha, 2010. Characterization of γ- and α-Fe_2O_3 nano powders synthesized by emulsion precipitation-calcination route and rheological behaviour of α-Fe_2O_3. *International Journal of Engineering, Science and Technology*, 2(8): 118-126.

Sears, W.G., 1956. Determination of Specific surface area of Colloidal silica by titration with sodium hydroxide. *Journal of analytical chemistry*, 28(12): 1981-1983.

Shaheen, W.M., and Hong, K.S., 2002. Thermal characterization and physicochemical properties of Fe_2O_3-Mn_2O_3/Al_2O_3 system. *Thermochimica Acta*, 381: 153-164.

Shihabudheen, M., S.M. Maliyekkal, K. AtulSharma, P.Ligy, 2006. Manganese-oxide-coated alumina: A promising sorbent for defluoridation of water. *Journal of Water Research*, 40: 3497-3506.

Sujana, M.G and Anand, S., 2010. Iron and aluminum based mixed hydroxides:A novel sorbents for fluoride removal form aqueous solution. *Journal of Applied Surface Science,* 256: 6956-6962.

Sujana, M.G. and Anand, S., 2010. Fluoride removal studies from contaminated ground water by using bauxite. *Desalination*, 267(2-3): 222-227.

Taddesse, A.M., A.S. Claassens & P.C. de Jager, 2008. Long-term kinetics of phosphate desorption from soil and its relationship with plant growth. *South Africa Journal of Plant Soil,* 25(3): 131-13.

Van der zee, S.E.A.T.M., L.G.J. Fokkink and W.H.A.Van Reimsdijk, 1987. A new technique for assessment of reversibly absorbed phosphate. *Soil Science Society of America Journal,* 51: 599-604.

Wang, Y., X.L. Zhao and J.L. Yan, 2004. An application of nano-technology in environmental protection. *Shanghai Enviromental Science*, 23(4): 178-181.

Zhang, G., H. Liu, R. Liu and J. Qu, 2009. Removal of phosphate from water by a Fe–Mn binary oxide adsorbent. *Journal of Colloidal and Interface Science*, 335: 168–174.

Zhao, X., J. Wang, F. Wu, Th.Wang, Y.Cai, Y. Shi and G. Jiang, 2010. Removal of fluoride from aqueous media by Fe-Al magnetic nanoparticles. *Journal of Hazardous Materials,* 173:102-109.

Zhong, X, B. Yang, X. Zhang, J. Jia and G. Yi, 2012. Effect of calcining temperature and time on the characteristics of Sb-doped SnO_2 nanoparticles synthesized by the sol–gel method. *Particuology,* 10(3): 365-370.

The IISTE is a pioneer in the Open-Access hosting service and academic event management. The aim of the firm is Accelerating Global Knowledge Sharing.

More information about the firm can be found on the homepage:
http://www.iiste.org

CALL FOR JOURNAL PAPERS

There are more than 30 peer-reviewed academic journals hosted under the hosting platform.

Prospective authors of journals can find the submission instruction on the following page: http://www.iiste.org/journals/ All the journals articles are available online to the readers all over the world without financial, legal, or technical barriers other than those inseparable from gaining access to the internet itself. Paper version of the journals is also available upon request of readers and authors.

MORE RESOURCES

Book publication information: http://www.iiste.org/book/

Academic conference: http://www.iiste.org/conference/upcoming-conferences-call-for-paper/

IISTE Knowledge Sharing Partners

EBSCO, Index Copernicus, Ulrich's Periodicals Directory, JournalTOCS, PKP Open Archives Harvester, Bielefeld Academic Search Engine, Elektronische Zeitschriftenbibliothek EZB, Open J-Gate, OCLC WorldCat, Universe Digtial Library , NewJour, Google Scholar